Tellus (1992), *44A*, 357–365

Semi-annual oscillation of the global divergent circulation

By TSING-CHANG CHEN and KUANG-DER WU, *Atmospheric Science Program, Department of Geological and Atmospheric Sciences, Iowa State University, Ames, IA 50011, USA*

(Manuscript received 1 October 1991; in final form 8 April 1992)

ABSTRACT

The multi-year outgoing long-wave radiation (OLR) and velocity potential (χ) generated from the 200-mb wind fields of the National Meteorological Center and the European Centre for Medium-Range Weather Forecasts were used to examine the structure of the semi-annual divergent circulation and its relation with tropical cumulus convection. As inferred from the semi-annual mode of the asymmetric OLR component (OLR_E), the east–west differential response to the solar heating between the Asian–Australian (AA) monsoon (60° E–120° W) and the extra-AA monsoon (120° W–60° E) hemispheres sustains a distinct semi-annual mode of the asymmetric divergent circulation with a wavenumber-1 structure. This semi-annual mode of the asymmetric divergent circulation, represented by the asymmetric velocity potential (χ_E), develops in time coherently with the semi-annual mode of tropical cumulus convection, which indicates a faster response in the extra-AA monsoon hemisphere. That is, the negative centers of semi-annual OLR_E anomalies and the divergent center of the semiannual χ_E field appear in the extra-AA monsoon hemisphere in April/October and in the AA-monsoon hemisphere in January/July.

1. Introduction

It was some two decades ago that Van Loon and Jenne (1969) analyzed the semi-annual oscillations of wind and temperature in the tropics of the Southern Hemisphere. They found a noticeable longitudinal asymmetry of these oscillations, stronger in the eastern than in the western hemisphere. Later, Van Loon and Jenne (1970) suggested that the semiannual oscillation over the eastern hemisphere is induced by the north–south shift of the local Hadley circulation. By comparing the semi-annual components of the outgoing long-wave radiation (OLR) and the 250-mb zonal wind, Weickmann and Chervin (1988) hypothesized that an east–west mass circulation should exist in association with the semi-annual cycle of OLR. However, a consistent depiction of the semi-annual OLR anomalies and the global divergent circulation does not emerge from these previous studies. It is our intent in this paper to report our recent finding concerning this particular issue, revealed from the analysis of the 200-mb divergent circulation and OLR data for the time period of 1979–1986.

2. Data and computations

The data used in this study were derived from 3 sources for the time period of 1979–1986.

(a) The OLR data,

(b) The 200-mb wind fields generated by the Global Data Assimilation System (GDAS) of the National Meteorological Center (NMC).

(c) The 200-mb wind fields generated by the GDAS of the European Centre for Medium Range Weather Forecasts (ECMWF).

In order to avoid the 1982/83 El Niño/Southern Oscillation (ENSO) effect on the semiannual oscillations of the divergent circulation and the OLR, our analysis does not include the time period from July 1982 to June 1983. As pointed out by Lambert (1989), both the NMC and ECMWF GDAS have been continuously updated in the past decade. For example, the ECMWF GDAS has two significant changes; the nonlinear diabatic normal-mode initialization was introduced in September 1983, and new physical parameterizations were implemented in May 1985. Apparently, the intensity of divergent circulation contained in the

Tellus A/44/5-1

assimilated data is changed. It was found that the divergent circulation generated with the ECMWF-GDAS data is much weaker between 1980 and 1981. We therefore used the ECMWF data only from January 1979–December 1979 and 1983–1986.

The divergent circulation is generally portrayed with velocity potential (χ). It was revealed from our previous study (Chen et al., 1988) that the annual and the 30–60 day oscillation modes individually explain about 40% variance of the χ departure from its annual mean. To prevent the appearance of 30–60 day oscillation from our analysis, we used the monthly-mean data, instead. On the other hand, the time variation of the monthly-mean data is dominated over most of the globe by the annual mode. To reduce the possible blending of the annual and semiannual modes in our analysis, we first remove the multiyear-mean and annual components from the monthly-mean χ and OLR fields in terms of a simple harmonic analysis. As inferred from studies of Van Loon and Jenne (1970) and Weickmann and Chervin (1988), the semi-annual components of divergent circulation and cumulus convection in the tropics may be induced by the east–west differential heating. It thus appears that we should focus our analysis on the asymmetric components of these two fields; i.e., χ_E and OLR_E, where $(\ )_E = (\ ) - (\ )_Z$ and $(\ )_Z$ is the zonal-mean $(\ )$. To isolate the semiannual components of χ_E and OLR_E, the empirical orthogonal function (EOF) analysis was adopted in this study. The advantage of this approach is that the selected eigenmode provides a spatial correlation between the semiannual cycle of a given variable in different geographic locations. Since the tropical OLR_E anomalies may reflect deep cumulus convection, we shall concentrate our analysis on the 200-mb χ_E field.

3. Results and discussion

If the semi-annual oscillation is stronger in the tropics of the eastern hemisphere and an east–west mass circulation can be induced by the semi-annual component of east–west differential heating, a seesaw semi-annual oscillation of convection and planetary-scale divergent circulation between the eastern and western hemispheres may exist. As revealed from rainfall climatology (e.g., Jaeger, 1976), the major precipitation of the globe occurs in the Asian–Australian (AA) monsoon region. To explore the seesaw semi-annual oscillation suggested above, time series of hemispheric-mean monthly OLR_E and χ_E averaged between 40°S and 40°N are shown in Fig. 1 for two hemispheres: the AA-monsoon (60°E–120°W) and the extra-AA monsoon (120°W–60°E). Several salient features emerge from these time series.

(a) The hemispheric-mean values of OLR_E and χ_E (solid lines) are always negative (positive) in the AA (extra-AA) monsoon hemisphere. The sign persistency of hemispheric-mean OLR_E and χ_E indicates that cumulus convection should be more active in the AA monsoon hemisphere, and the divergent center of χ_E should be located in this hemisphere, too. The latter situation will later be illustrated further.

(b) The semi-annual variations of hemispheric-mean OLR_E and χ_E stand out clearly by contrasting the semi-annual harmonics (dashed lines) and real time series of these two quantities. The expected see-saw semi-annual oscillations of convection and planetary-scale divergent circulation between the AA- and the extra-AA monsoon hemispheres are confirmed by the fact that either hemispheric-mean OLR_E or χ_E in the two hemispheres vary oppositely in time. Interestingly, hemispheric-mean OLR_E and χ_E of the same hemisphere vary temporarily in phase.

The in-phase semi-annual oscillations between hemispheric-mean OLR_E and χ_E may be explained in the following. It was shown by diagnostic analysis of the heat budget (e.g., Chen and Baker, 1987; Holton, 1979) that the tropical diabatic heating is primarily counterbalanced by adiabatic cooling, i.e.,

$$-\sigma\omega \simeq \frac{1}{C_p}\dot{Q}, \tag{1}$$

where σ is static stability, ω p-vertical velocity, C_p specific heat of constant pressure and $\dot{Q}$ diabatic heating. Combining (1) with the continuity equation, one can easily find that

$$\chi \simeq \nabla^{-2}\left[\frac{\partial}{\partial p}\left(\frac{1}{C_p\sigma}\dot{Q}\right)\right] \tag{2}$$

in the tropics. The latent heat released by cumulus

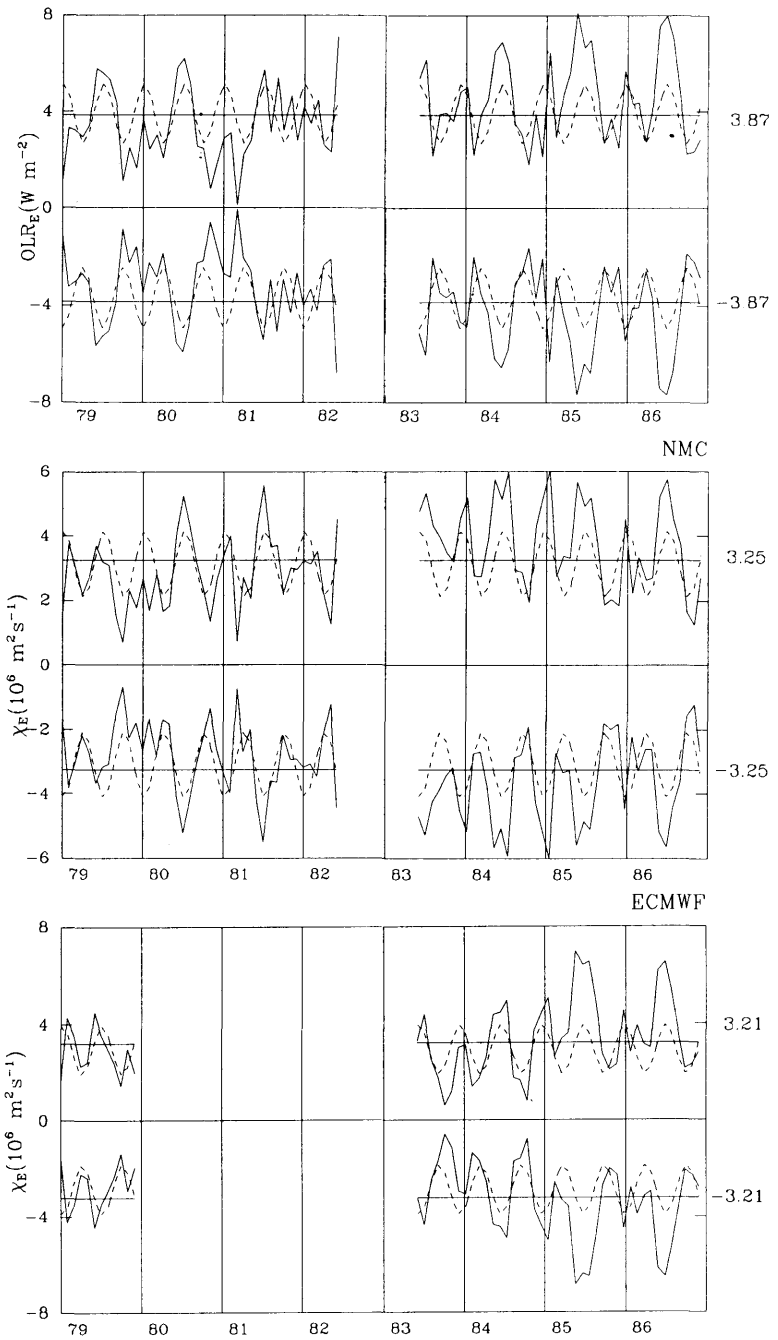

Fig. 1. Time series (solid line) of the hemispheric-mean monthly OLR_E and χ_E (200 mb) fields of 2 hemispheres: the Asian–Australian (AA) monsoon (60°E–120°W, lower lines of each panel) and the extra-AA monsoon (120°W–60°E, upper lines of each panel). The semi-annual harmonic (dashed line) of each quantity is also included. The straight solid line represents the multi-year-mean value of each quantity shown on the right of each panel. The χ_E (200 mb) fields were generated from the NMC and ECMWF data.

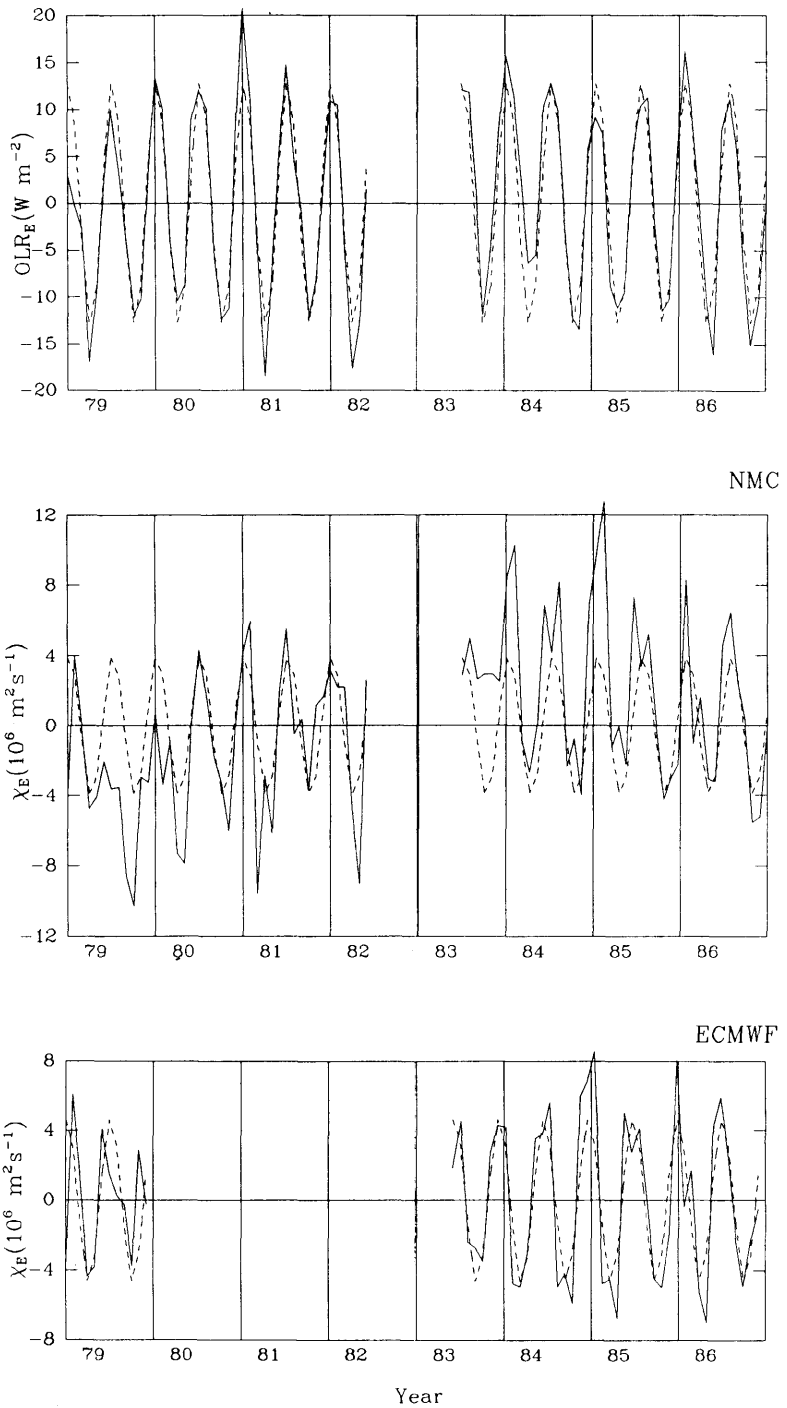

Fig. 2. Eigen-coefficient time series (solid lines) of the first non-annual eigen-mode of OLR_E, χ_E(NMC) and χ_E(ECMWF), with semi-annual harmonics (dashed lines).

convection constitutes the major part of tropical diabatic heating. The in-phase semi-annual oscillations between the hemispheric-mean OLR_E and χ_E shown in Fig. 1 can be realized through (2).

As shown in Fig. 1, the see-saw semi-annual oscillations of the hemispheric-mean OLR_E and χ_E exist between the AA and the extra-AA monsoon hemispheres. However, one may question whether these see-saw semi-annual oscillations are really global and what may be the cause of these oscillations. In order to shed some light on these questions, we have to understand the time evolution of the horizontal structure of the semi-annual OLR_E and χ_E components. Following the procedure outlined in Section 2, we performed the EOF analysis of these 2 variables over the globe to serve this purpose. The variance (VE) contributed by the 1st leading eigenmodes of the non-annual OLR_E anomalies and the semi-annual fractional variance of these eigenmodes are displayed in Table 1. As revealed from the eigen-coefficient time series (solid lines) and fractional variances of the semi-annual harmonics (dashed lines) shown in Fig. 2, the semi-annual components of OLR_E and χ_E are well represented by the first leading eigen-modes of these two variables.

The eigen-coefficient time series of OLR_E and χ_E are almost temporarily in phase. This close correlation between these time series indicates that the semi-annual modes of OLR_E and χ_E oscillate in a coherent manner. The χ_E eigen-vectors of both NMC and ECMWF data (Fig. 3) exhibit a wavenumber-1 structure; a center located in the AA-monsoon hemisphere, and another one of opposite sign over the extra-AA monsoon hemisphere. In contrast, multiple centers appear in the OLR_E eigenvector; the major positive centers are located in the westernmost Pacific and the Indian Ocean, and the major negative centers in tropical South America and equatorial Africa. In fact, the χ_E and OLR_E eigen-vectors are relatively consistent in the sense that their major centers of opposite signs coincide. The divergent (convergent) center of the upper-level divergent circulation is depicted by the negative (positive) center of χ_E. According to (2), it is expected that the negative (positive) χ_E center coincides with the positive (negative) center of vertical differential heating. Based upon this argument, it is not surprising that the negative (positive) χ_E center matches well with the OLR_E center of opposite sign.

Table 1. *Variance (VE) explained by the most significant non-annual eigen-modes of the OLR_E and χ_E anomalies, in which the multi-year mean and annual components were removed by a simple harmonic analysis and the semi-annual fractional variance (FE) of these eigen-modes; the phase denotes the date (month/day) when the semi-annual harmonic of the eigen-coefficient time series reaches its first maximum value*

Variable	VE (%)	Semi-annual FE (%) (phase)
OLR	12.6	88.3 (1/14)
$\chi_{200\,mb}$(NMC)	51.9	48.0 (1/11)
$\chi_{200\,mb}$(ECMWF)	56.3	60.4 (1/7)

In order to facilitate discussions of the characteristics and physical functions of semi-annual OLR_E and χ_E cycles in the physical domain, we prepare the time-average maps of these two variables by multiplying the first leading eigen-vector with the corresponding eigen-coefficients. It is revealed from the time series of eigen-coefficients shown in Fig. 2 that semi-annual OLR_E and χ_E modes reach their minimum and maximum amplitudes about 1 month after the equinox and the solstice, respectively. For these two special times, we thus prepare synoptic maps of the semi-annual OLR_E and χ_E modes and also superimpose $\nabla\chi_E$ vectors on χ_E to indicate centers of convergence and divergence. Shown in Figs. 4 and 5 are the semi-annual χ_E anomalies of the NMC and ECMWF data, respectively, with the semi-annual OLR_E anomalies for January/July and April/October.

During April/October a convergent center of the semi-annual χ_E mode is located in the western equatorial Pacific and a divergent center over the equatorial Atlantic (Figs. 4b and 5b). Apparently, an ascending branch of the semi-annual divergent circulation resides over the equatorial, *land-dominated* (extra-AA monsoon: South America/Africa) hemisphere, and a descending branch resides over the equatorial *water-dominated* (AA-monsoon: the Indian Ocean/the Western Pacific) hemisphere. The distribution of the semi-annual OLR_E anomalies is consistent with that of the semi-annual χ_E anomalies in such a way that during April/October the land-dominated

hemisphere becomes more convectively active and the water-dominated hemisphere less convectively active. The entire synoptic structures of the semi-annual OLR_E and χ_E anomalies are reversed during January/July (Figs. 4b and 5b).

Weickmann and Chervin (1988) pointed out that the semi-annual component contributes about 63% of the incoming solar heating at the equator. This significant radiative forcing should induce an atmospheric response. Note that this semi-annual solar heating becomes insignificant about 10° latitude away from the equator. However, Van Loon (1967) and Meehl (1991) showed that the heat storage of the oceans delays the summer temperature maximum and winter minimum at the ocean. White and Wallace (1978) also argued that the late summer maximum at the sea surface temperature is sharper than the late winter minimum; a semi-annual component of the surface temperature is resulted from this seasonally thermal asymmetry. On the other hand, the convective activities over land follow closely the seasonal match with their maximum during the warm season. It is likely that both the *direct* radiative forcing of the semi-annual solar heating at the equator and the *indirect* thermal process related to the heat storage of the ocean in response to the annual solar heating work coherently in the tropics to shape the cumulus convection and divergent circulation as observed in this study.

The contrast of the semi-annual OLR_E and χ_E anomalies during the solstice (Figs. 4a and 5a) and

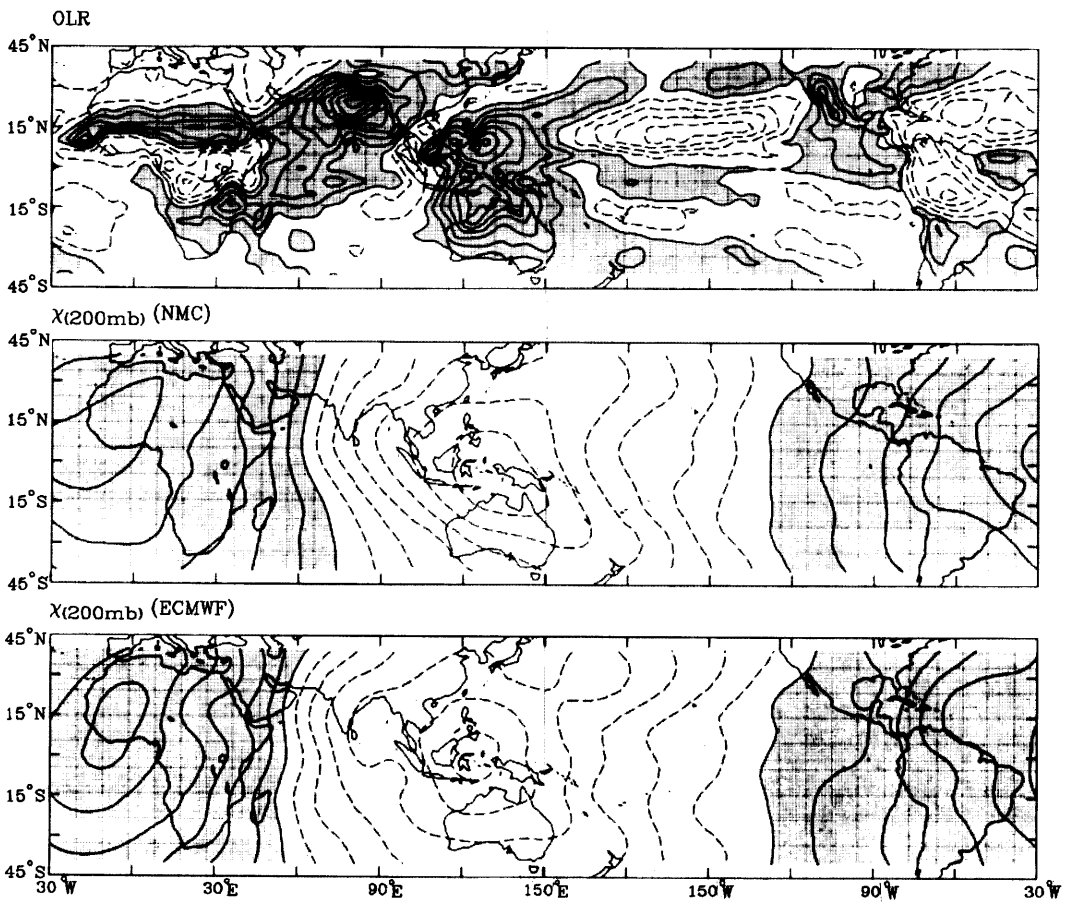

Fig. 3. Eigen-vectors corresponding to eigen-coefficient time series shown in Fig. 1. The positive values are shaded. The contour interval of eigen-vectors is 0.1.

the equinox (Figs. 4b and 5b) reveals clearly that a differential response of the atmosphere to the solar heating exists between the land- and water-dominated hemispheres; the land (water)-dominated hemisphere gains negative (positive) semi-annual OLR_E anomalies in spring and fall, and the water (land)-dominated hemisphere attains negative (positive) semi-annual OLR_E anomalies in summer and winter. These comparisons reveal clearly that the equatorial land-dominated hemisphere responds faster to the solar heating than the equatorial water-dominated hemisphere. According to (2), the semi-annual east–west divergent circulation should be induced by the east–west differential heating between the land- and water-dominated hemispheres. A better view of the see-saw semi-annual oscillation of the divergent circulation between these two hemispheres may be gained from the $x-t$ diagrams of the semi-annual χ_E anomalies at the equator (not shown). The alternation of convergent and divergent cells, indicated respectively by the positive and negative semi-annual χ_E anomalies, between the land-dominated (AA monsoon) and the water-dominated (extra AA monsoon) hemispheres takes place *twice* a year. Our analysis of the semi-annual χ_E and OLR_E mode substantiates Weickmann and Chervin's (1988) suggestion that an east–west mass circulation may be induced by the response of the atmosphere to the east–west differential heating between these two hemispheres.

Besides the semi-annual components of the global divergent circulation and tropical cumulus convection, a regional feature is worth noting. Van Loon suggests that the semi-annual oscillation of temperature over the tropical region between 60° E and 120° E is caused by the north–south migration of the local Hadley circulation. As shown in Figs. 4 and 5, the semi-annual divergent circulation converges (diverges) towards (out of) the major minimum (maximum) centers of semi-annual OLR_E anomalies, north and south of the equator over the Australian longitudes during April/October

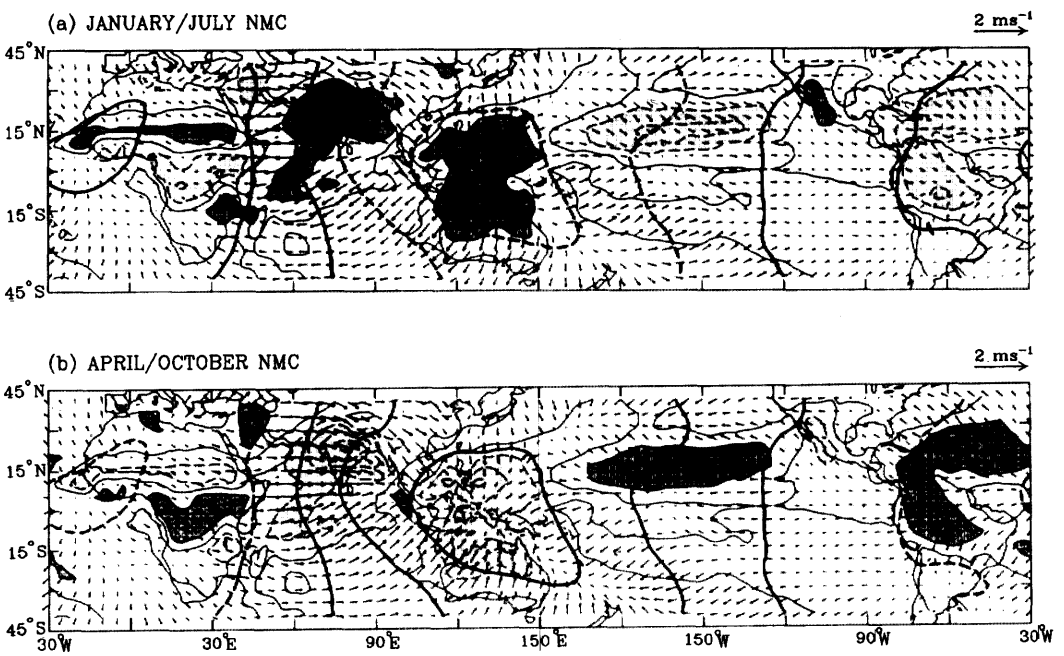

Fig. 4. (a) January/July and (b) April/October semi-annual components of the (χ_E, V_{DE}) and OLR_E anomalies. Note that $V_{DE} = \nabla\chi_E$. The contour intervals of semi-annual χ_E (thick lines) and OLR_E (thin lines) are 2×10^5 m^2 s^{-1} and 5 W m^{-2}, respectively. The areas with the semi-annual OLR_E anomaly $\leqslant -5$ W m^{-2} are heavily shaded, while those with the semi-annual OLR_E anomaly $\geqslant 5$ W m^{-2} are lightly shaded. The χ_E fields were generated from the 200-mb wind data of the NMC GDAS.

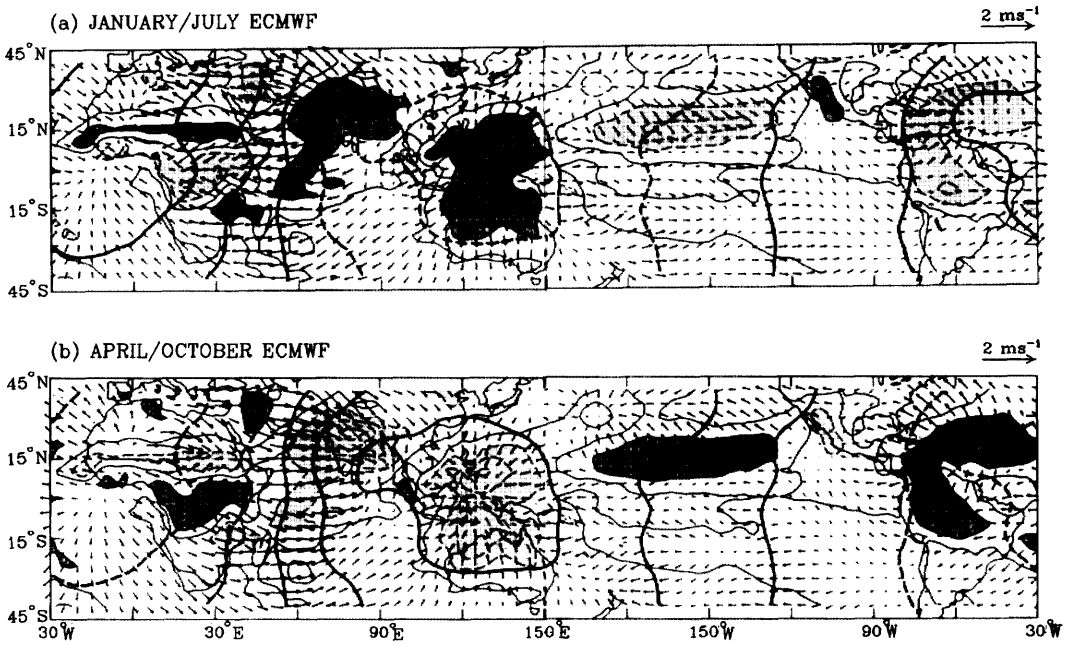

Fig. 5. Same as Fig. 4, except the χ_E fields were generated from 200-mb wind data of the ECMWF GDAS.

(January/July). Suppose that the latent heat released by cumulus convection contributes significantly to temperature over this region. One can then expect negative (positive) temperature perturbation over this region during April/October (January/July). This argument is relatively consistent with Van Loon and Jenne's analysis (1970, their Figs. 3–5). Their observations of the semi-annual temperature oscillation can therefore be explained by the semi-annual cycle of cumulus convection and divergent circulation depicted in this study.

4. Concluding remarks

It was revealed from previous studies that the direct semi-annual solar heating is significant at the equator and the heat storage of the ocean delays the summer maximum and winter minimum of the ocean temperature in response to the annual solar heating. Since the seasonal march of land heating follows closely the solar heating, Weickmann and Chervin (1988) suggested that an east–west circulation and cumulus convection in the tropics can be induced by the different heating between land- and ocean-dominated hemispheres. The OLR data are often used as the proxy of cumulus convection, and velocity potential χ is always employed to portray divergent circulation. Performing the EOF analysis of the multi-year OLR_E and χ_E data, we are able to depict the time evolution of and the relation between the semi-annual modes of cumulus convection and divergent circulation in the tropics. Our major findings in this study are as follows.

(a) The semi-annual χ_E anomalies exhibit a well organized wavenumber-1 structure with a center in the Asian–Australian (AA) monsoon hemisphere (60°E–120°W) and a center of opposite sign in the extra-AA monsoon hemisphere (120°W–60°E). The divergent (convergent) center of the semi-annual asymmetric divergent circulation coincides with the major negative (positive) centers of the semi-annual OLR_E component.

(b) As indicated by the time evolution of the semi-annual OLR_E anomalies, the extra-AA monsoon (equatorial land-dominated) hemisphere

responds faster to the solar heating than the AA monsoon (equatorial water-dominated) hemisphere; the major negative centers of the maximum semi-annual OLR_E anomalies appear in the former hemisphere in April/October and in the latter hemisphere in January/July. It was inferred that the semi-annual χ_E mode is sustained by two forcings: the east–west differential response of tropical cumulus convection to the semi-annual radiative forcing between the two hemispheres and the delay of the summer temperature and winter minimum at the ocean by the heat storage of the ocean.

The annual and semi-annual modes of the atmospheric circulation are the most pronounced short-term climate signals. In the past decades, the full-physics general circulation model has been used in many research centers to simulate the global climate change. However, it may be difficult to use model simulations to determine the mechanism causing the climate change if the relatively regular annual and semi-annual modes of the atmospheric circulation cannot be properly simulated. Recently, numerous attentions have been attracted to investigate various aspects of the annual-cycle component of the atmospheric circulation. Unfortunately, few attempts have been made to analyze the semi-annual mode. The major effort of this study not only explores the structure of the semi-annual divergent circulation and its relation with tropical cumulus convection, but also provides some general circulation statistics for the verification of the semi-annual divergent circulation simulated by climate models.

Acknowledgements

This study is supported by the NSF Grants ATM-8912451 and ATM-9141537. The major data processing of this study was performed on the YMP supercomputer of the National Center for Atmospheric Research, which is sponsored by the National Science Foundation. We appreciate the typing assistance provided by Mrs. Reatha Diedrichs.

REFERENCES

Chen, T.-C. and Baker, W. E. 1986. Global diabatic heating during FGGE SOP-1 and SOP-2. *Mon. Wea. Rev. 114*, 2578–2589.

Chen, T.-C., Tzeng, R.-Y. and Yen, M.-C. 1988. Development and life cycle of the Indian monsoon: Effect of the 30–50 day oscillation. *Mon. Wea. Rev. 116*, 2183–2199.

Holton, J. R. 1978. *An introduction to dynamic meteorology*. Academic Press, 391 pp.

Jaeger, L. 1976. Monatskarten des Niederschlags für die ganze Erde. *Ber. Dt. Wetterd 18*, 139, 38 pp.

Lambert, S. J. 1989. A comparison of divergent winds from the National Meteorological Center and the European Center for Medium Range Weather Forecasts global analysis for 1980–1986, *Mon. Wea. Rev. 117*, 995–1005.

Meehl, G. A. 1991. A reexamination of the mechanism of the semi-annual oscillation in the Southern Hemisphere. *J. Climate 9*, 911–926.

Van Loon, H. 1967. The half-yearly oscillation in middle and high southern latitudes and the coreless winter. *J. Atmos. Sci. 24*, 472–486.

Van Loon, H. and Jenne, R. L. 1969. The half-yearly oscillation in the tropics of the Southern Hemisphere. *J. Atmos. Sci. 26*, 218–232.

Van Loon, H. and Jenne, R. L. 1970. On the half-yearly oscillation in the tropics. *Tellus 22*, 391–398.

Weickmann, K. M. and Chervin, R. M. 1988. The observed and simulated atmospheric cycle. Part I: Global wind fields models. *J. Climate 1*, 265–289.

White, G. H. and Wallace, J. M. 1978. The global distribution of the annual and semi-annual cycles in surface temperature. *Mon. Wea. Rev. 106*, 901–906.